

RESEARCH

Open Access



# Immunogenomic intertumor heterogeneity across primary and metastatic sites in a patient with lung adenocarcinoma

Runzhe Chen<sup>1,2,3†</sup>, Jun Li<sup>2,4†</sup>, Junya Fujimoto<sup>5</sup>, Lingzhi Hong<sup>1</sup>, Xin Hu<sup>2</sup>, Kelly Quek<sup>1,2</sup>, Ming Tang<sup>2</sup>, Akash Mitra<sup>2</sup>, Carmen Behrens<sup>1</sup>, Chi-Wan Chow<sup>5</sup>, Peixin Jiang<sup>1</sup>, Latasha D. Little<sup>2</sup>, Curtis Gumbs<sup>2</sup>, Xingzhi Song<sup>2</sup>, Jianhua Zhang<sup>2</sup>, Dongfeng Tan<sup>6</sup>, John V. Heymach<sup>1</sup>, Ignacio Wistuba<sup>5</sup>, P. Andrew Futreal<sup>2</sup>, Don L. Gibbons<sup>1\*</sup>, Lauren A. Byers<sup>1\*</sup>, Jianjun Zhang<sup>1,2\*</sup> and Alexandre Reuben<sup>1\*</sup> 

## Abstract

**Background:** Lung cancer is the leading cause of cancer death, partially owing to its extensive heterogeneity. The analysis of intertumor heterogeneity has been limited by an inability to concurrently obtain tissue from synchronous metastases unaltered by multiple prior lines of therapy.

**Methods:** In order to study the relationship between genomic, epigenomic and T cell repertoire heterogeneity in a rare autopsy case from a 32-year-old female never-smoker with left lung primary late-stage lung adenocarcinoma (LUAD), we did whole-exome sequencing (WES), DNA methylation and T cell receptor (TCR) sequencing to characterize the immunogenomic landscape of one primary and 19 synchronous metastatic tumors.

**Results:** We observed heterogeneous mutation, methylation, and T cell patterns across distinct metastases. Only TP53 mutation was detected in all tumors suggesting an early event while other cancer gene mutations were later events which may have followed subclonal diversification. A set of prevalent T cell clonotypes were completely excluded from left-side thoracic tumors indicating distinct T cell repertoire profiles between left-side and non left-side thoracic tumors. Though a limited number of predicted neoantigens were shared, these were associated with homology of the T cell repertoire across metastases. Lastly, ratio of methylated neoantigen coding mutations was negatively associated with T-cell density, richness and clonality, suggesting neoantigen methylation may partially drive immunosuppression.

**Conclusions:** Our study demonstrates heterogeneous genomic and T cell profiles across synchronous metastases and how restriction of unique T cell clonotypes within an individual may differentially shape the genomic and epigenomic landscapes of synchronous lung metastases.

**Keywords:** Lung adenocarcinoma, Intertumor heterogeneity, Genomic, T cell repertoire

<sup>†</sup>Runzhe Chen and Jun Li are co-first authors.

\*Correspondence: [dlgibbon@mdanderson.org](mailto:dlgibbon@mdanderson.org); [lbyers@mdanderson.org](mailto:lbyers@mdanderson.org); [jzhang20@mdanderson.org](mailto:jzhang20@mdanderson.org); [areuben@mdanderson.org](mailto:areuben@mdanderson.org)

<sup>1</sup> Department of Thoracic/Head and Neck Medical Oncology, the University of Texas MD Anderson Cancer Center, Houston, TX 77030, USA

<sup>2</sup> Department of Genomic Medicine, the University of Texas MD Anderson Cancer Center, Houston, TX 77030, USA

Full list of author information is available at the end of the article

## Background

Lung cancer is the leading cause of cancer death, partially owing to its extensive heterogeneity [1, 2]. It has been proposed that this extensive heterogeneity results from successive clonal expansion and selection of the fittest clones influenced by genomic accumulation and somatic epigenetic alterations [3–6]. However, tumor evolution



may also be shaped by pressure from the immune system, which can prune the most immunogenic branches of the tumor [7].

T cells play a crucial role in preventing cancer development through antigen-specific detection and destruction of malignant cells, though evolving tumors can eventually escape immune surveillance through a process termed immunoediting [4, 8–11]. Few studies have addressed the impact of the T cell repertoire in shaping metastatic heterogeneity [12–14] with most work to date evaluating longitudinal changes spanning multiple time-points and therapies. Though these studies offer crucial insights, they do not allow the evaluation of intrinsic intertumor heterogeneity in absence of selective pressure from therapy. Furthermore, to date, the analysis of intertumor heterogeneity has been limited by an inability to concurrently obtain tissue from synchronous metastases unaltered by multiple prior lines of therapy [15–17].

Here, we sought to study the relationship between genomic, epigenomic and T cell repertoire heterogeneity in a rare autopsy case from a 32-year-old female never-smoker with left lung primary late-stage lung adenocarcinoma (LUAD) with more than 20 synchronous metastases. We observed heterogeneous mutation, methylation, and T cell patterns across distinct metastases including a set of prevalent T cell clonotypes which were completely excluded from left-side thoracic tumors. Our work further highlights neoantigen methylation as a potential mechanism driving immunosuppression and some of the hurdles facing the treatment of late-stage lung cancer.

## Methods

### Human subject research

We collected 20 tumor samples and one normal gastrointestinal (GI) tract sample at autopsy. Collection and use of patient samples were approved by the Institutional Review Board of the University of Texas MD Anderson Cancer Center. Clinical information is presented in Supplementary Table 1.

### Sample collection

DNA of collected samples was isolated from FFPE tissues using the AllPrep DNA/RNA FFPE Kit (Qiagen, Hilden, Germany). Hematoxylin and eosin (H&E) slides of each case were reviewed by experienced lung cancer pathologists under the microscope to assess the percentage of tumor tissues versus normal tissues. Tumor cell viability was also assessed by examining the presence of necrosis in the tissues. Only samples with enough viable tumor cells were selected for whole-exome sequencing (WES), methylation and immunoSEQ.

### DNA preparation

Unstained tissue sections (10  $\mu$ m thick) were deparaffinized in xylene and 100% ethanol (twice in each for 10 minutes). The macrodissected tumor areas of the deparaffinized tissues were placed into 1.5 mL collection tubes for DNA extraction. The tissue was next suspended with Buffer PKD and Proteinase K from the Allprep FFPE kit. After incubating at 56°C for 15 min and on ice for 5 min, the mixed solution was centrifuged for 15 minutes at 20,000  $\times$  g. Finally, the DNA samples were quantified by Nano Drop 1000 Spectrophotometer (Thermo Scientific, Wilmington, DE, USA). The fragmentation sizes were evaluated by the Agilent 2200 Tape Station system using the Genomic DNA Screen Tape Assay (Agilent Technologies, Santa Clara, CA, USA).

### Whole-exome sequencing

Exome capture was performed on 500 ng of genomic DNA per sample based on KAPA library prep (Kapa Biosystems) using the Agilent SureSelect Human All Exon V4 kit according to the manufacturer's instructions and paired-end multiplex sequencing was performed on the Illumina HiSeq 2000 sequencing platform. The average sequencing depth was 178x (ranging from 63x to 225x, standard deviation  $\pm$  31).

### Mutation calling

Tumor contents and major/minor copy number changes were estimated by Sequenza (v2.1.2) [18]. To control those FFPE caused artifact contaminations, somatic single nucleotide variants (SNVs) was first called using MuTect version 1.1.4 [19], VarScan 2 [20] and Strelka2 [21] with default setting, respectively. Then, the following filtering criteria were applied to each callers: 1) sequencing depth  $\geq 20\times$  in tumor DNA and  $\geq 10\times$  in germline DNA; 2) variant allele frequency (VAF)  $\geq 0.02$  in tumor DNA and  $< 0.01$  in germline DNA; 3) the total number of reads supporting the variant calls is  $\geq 4$ ; and 4) variant frequency is  $< 0.01$  in ESP6500, 1000 genome and EXAC databases. Mutations called by Mutect with a LOD score  $< 10$  were further filtered out, and those mutations called by Strelka with a quality score below 35 was also filtered out. Finally, only those mutations were kept if called by any of the two tools and rescued if any were rejected but shared by at least two tumors. Identified missense mutations were manually reviewed using the Integrative Genomics Viewer (IGV) version 2.3.61 [22, 23].

### Phylogenetic analysis

Ancestors were germline DNA assuming with no mutations. The phylogenetic tree was generated as described [24]. A binary presence/absence matrix of all somatic

mutations detected was used as input for R package phangorn version 2.0.2 [25].

### Neoantigen predictions

Nonsynonymous mutations were identified from WES profiling and the binding affinities with patient-restricted MHC Class I molecules of all possible 9- and 10-mer peptides spanning the nonsynonymous mutations were evaluated with the NetMHC3.4 algorithm based on HLA-A, HLA-B, and HLA-C alleles of each patient [26–28]. Candidate peptides were considered as HLA binders when  $IC_{50} < 500$  nM with high affinity binders presenting  $IC_{50} < 50$  nM.

### DNA methylation profiling and tumor-immune microenvironment deconvolution

Genomic DNA (approximately 500 ng) was bisulfite converted using EZ DNA Methylation Kit (Zymo Research Corp. Irvine, CA, USA) following the manufacturer's protocol. Bisulfite converted DNA materials were then processed and hybridized to the Infinium Human Methylation 450k arrays (Illumina, San Diego, CA, USA) according to manufacturer's recommendation. Preprocessing and initial quality assessments of the raw data were examined using the following R packages. Subset-quantile within-array normalization (SWAN) [29] was used to normalize raw methylation values. IlluminaHumanMethylation450k.db annotation package was used to annotate the CpG probes location. Probe sets with a beta value above 0.3 were taken as methylated [30, 31]. Before any genomic and statistical analyses were conducted, we normalized and inspected the methylation data for the presence of substantial confounding batch effects. Cellular deconvolution analyses were carried out using estimated cellular fractions using MethylCIBERSORT [32].

### TCR $\beta$ sequencing and comparison parameters

Immunosequencing of the CDR3 regions of human T cell receptor (TCR)  $\beta$  chains was performed using the protocol of immunoSEQ (Adaptive Biotechnologies, hsTCR $\beta$  Kit) [33–35]. Two sets of PCRs were performed on DNA extracted from the tissues collected. The initial PCR used a mix of multiplexed V- and J-gene primers which amplify all possible recombined receptor sequences from the DNA sample, and a second PCR designing to add unique DNA barcodes to each PCR product was followed. After that, samples were pooled together with a negative and a positive control. The pools were then sequenced on an Illumina MiSeq platform using 150 cycle paired-end protocol and sequence-ready primers. After finish the sequencing, the raw data were transferred to Adaptive Biotechnologies and processed into a report including those passed quality-check samples

and a normalized and annotated TCR $\beta$  profile repertoire accordingly. Profile of TCR rearrangements is presented in [Supplementary Data](#).

T-cell density in FFPE tissue samples was calculated by normalizing TCR- $\beta$  template counts to the total amount of DNA usable for TCR sequencing, where the amount of usable DNA was determined by PCR-amplification and sequencing of housekeeping genes expected to be present in all nucleated cells. T-cell richness is a metric of T cell diversity, and it is calculated by on the T-cell unique rearrangements. T-cell clonality is a metric of T cell proliferation and reactivity, and it is defined as 1-Peilon's evenness and is calculated on productive rearrangements by:

$$1 + \frac{\sum_i^N p_i \log_2(p_i)}{\log_2(N)}$$

where  $p_i$  is the proportional abundance of rearrangement  $i$ , and  $N$  is the total number of rearrangements. Clonality ranges from 0 to 1: values approaching 0 indicate a very even distribution of frequency of different clones (polyclonal), whereas values approaching 1 indicate a distinct asymmetric distribution in which a few activated clones are present at high frequencies (monoclonal). JI is conceptually a percentage of how many objects of two sets have in common out of how many objects they have in total.  $JI = (\text{number of rearrangements in common}) / (\text{total number of rearrangements})$ . Statistical analysis was performed in R version 3.2.

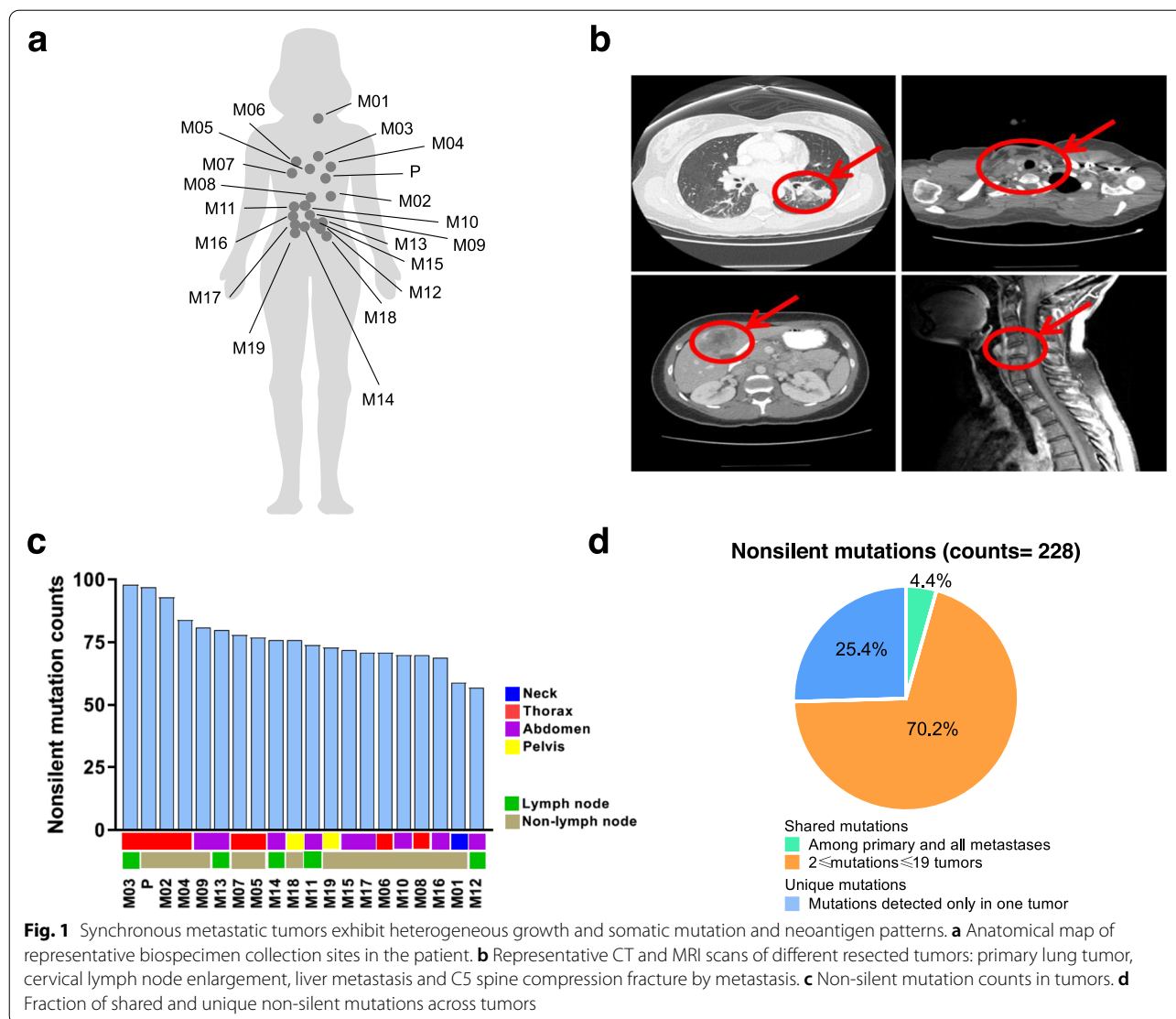
### Statistical Analysis

Graphs were generated with GraphPad Prism 8.0. Spearman's rank correlations were calculated to assess the association between 2 continuous variables. Kruskal-Wallis tests were used for categorical variables with more than 2 levels.  $P$ -values less than 0.05 were considered to be statistically significant.

## Results

### Patient information

A 32-year-old female never-smoker presented to her primary care physician complaining of weakness in her upper right arm lasting for two weeks. Physical examination was unremarkable, other than grade 3 weakness in her right upper limb. Shortly after, she was hospitalized due to acute venous thromboembolism of this arm. She was started on anti-coagulants and underwent computed tomography (CT) scans of the chest, abdomen and pelvis and magnetic resonance imaging (MRI) of the brain as part of the work up. Numerous nodules were detected suggestive of extensive metastasis and a 1.9 cm left lung mass was consistent with a lung primary origin (Fig. 1a,



b). A liver biopsy revealed the diagnosis of poorly differentiated LUAD. Core biopsy of left chest wall nodule also revealed poorly differentiated LUAD with tumor cells positive for pan-keratin and TTF-1 and negative for ER, PR, CDX2, WT1, PAX-8, synaptophysin and chromogranin. The patient underwent palliative radiation therapy for C5-C7 spine metastases with  $10 \times 300$  cGy and one dose of chemotherapy with carboplatin and paclitaxel while awaiting molecular profiling results. Her condition deteriorated rapidly and she expired 13 days following her sole dose of chemotherapy due to the disseminated metastatic cancer and cancer-associated complications including severe respiratory, cardiovascular and renal failure caused by Trousseau syndrome and embolic stroke despite continuing hydrocortisone combined with antibiotic therapy for the last two days preceding her death. An autopsy was

performed and widely disseminated metastatic carcinoma involving multiple systems and organs was observed.

To understand the genomic and T cell landscape of this extensively metastatic LUAD, 20 tumor samples (Supplementary Table 1) including the left lung (primary tumor, P), thyroid gland (M01), left pleural cavity (M02), left hilar lymph node (M03), left parietal pleura (M04), heart (M05), right lung (M06), right pleural cavity (M07), 12th thoracic vertebra (M08), gastrointestinal (GI) tract (M09), liver (M10), 4 abdominal lymph nodes (M11–14), left adrenal gland (M15), two metastases in the right kidney (M16 and M17), left and right ovaries (M18 and M19) as well as one histologically normal sample from the GI tract were collected and subjected to WES, DNA methylation array and TCR sequencing.

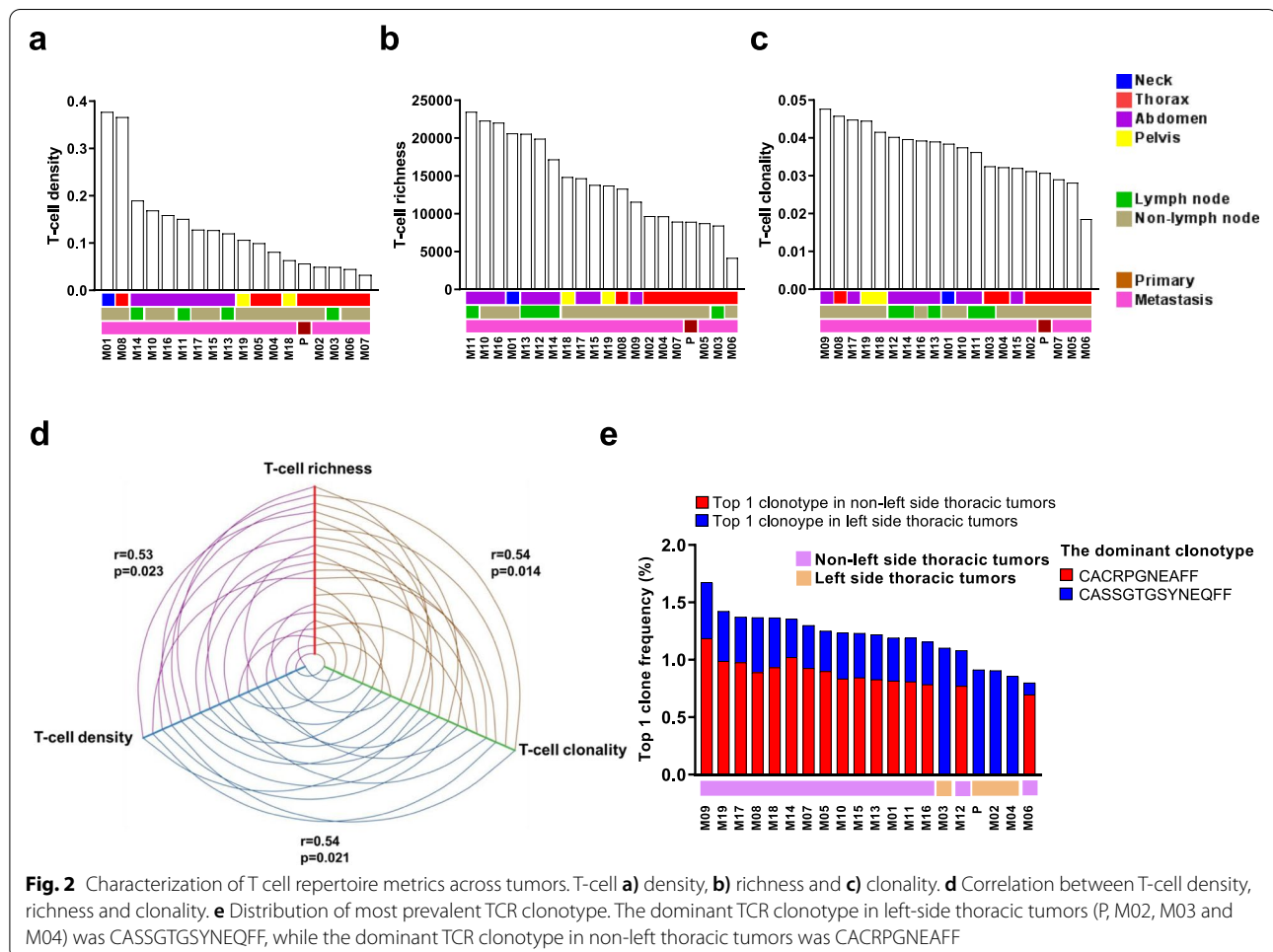
### Distinct mutational profiles are seen across primary tumor and synchronous metastases

Overall, 228 non-silent mutations were detected with an average of 76 per sample (range = 57–98). The number of non-silent mutations varied between tumors, with only 10 shared across all 20 samples (Fig. 1c). Of these non-silent mutations, 170 (75%) were shared by at least two tumors while 58 (25%) were unique (Fig. 1d). When canonical cancer gene mutations were analyzed [36–38], commonly-mutated cancer genes included TP53, CDKN2A, ASXL1 and MET in this patient (Supplementary Fig. 1a). Only TP53 mutation (chromosome 17\_7578382, stop gain, spectrum G->C) was detected in all tumors suggesting TP53 mutation was an early genomic event, while other cancer gene mutations were later events which may have followed subclonal diversification. We also constructed a phylogenetic tree to depict the genomic heterogeneity and evolutionary trajectory of these metastatic tumors. As shown in Supplementary Fig. 1b, the phylogenetic structure varied considerably between tumors highlighting profound genomic heterogeneity within this patient. We then

utilized the Jaccard index (JI), which takes into consideration the proportion of shared non-silent mutations between any two samples. The JI ranged from 0.14 to 0.82 (average = 0.49) with more proximal tumors generally more genetically similar (Supplementary Fig. 1c). Homology between the primary and metastases ranged from 0.14 to 0.73 (average = 0.33), with the thoracic lesions including the left pleural metastasis, left hilar lymph node and right pleural metastasis exhibiting the greatest similarity with the primary tumor. Taken together, these results reveal marked genomic heterogeneity across different metastases within the same patient.

### The T cell infiltrate in distant metastases is more dense, diverse and reactive

The crucial role of T cells in immunoeediting led us to study the T cell repertoire to further investigate the spatial heterogeneity of T-cell responses [39, 40]. T-cell density, an estimate of the proportion of T cells within a tumor, ranged from 3 to 38% (average = 13%, Fig. 2a), while richness, a measure of T-cell diversity, ranged from



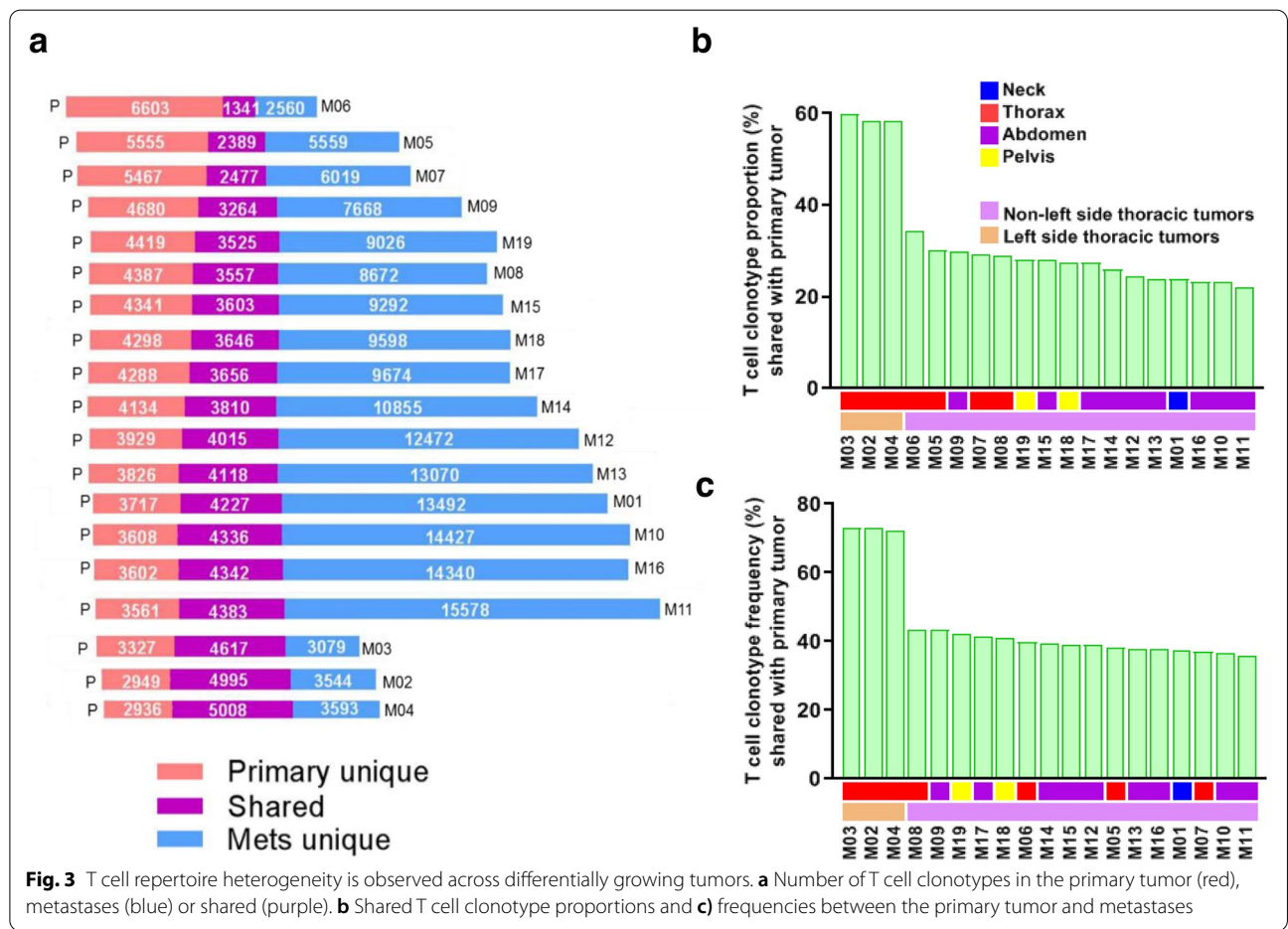
4,168 to 23,487 unique T-cell rearrangements (average=14,344 unique rearrangements, Fig. 2b). T-cell clonality, a measure of T-cell reactivity, ranged from 0.02 to 0.05 (average=0.04, Fig. 2c). All TCR metrics were positively inter-correlated (Density vs. Richness:  $r=0.53$ ,  $p=0.02$ ; Density vs. Clonality:  $r=0.54$ ,  $p=0.02$ ; Clonality vs. Richness:  $r=0.54$ ,  $p=0.01$ , Fig. 2d). Compared to prior work from our group in an early-stage LUAD cohort [41], lower T-cell density ( $p<0.05$ ) and clonality ( $p<0.0001$ ) and higher richness ( $p<0.0001$ ) were observed in tumors from this patient (Supplementary Fig. 2a-e).

Tumors were then grouped anatomically. Non-thoracic tumors displayed higher T-cell density ( $p<0.01$ ), richness ( $p<0.0001$ ) and clonality ( $p<0.01$ ) than thoracic tumors (Supplementary Fig. 3a-c), perhaps owing to their anatomical location away from the primary tumor and its immunosuppressive influences [42, 43]. Lymph nodes serve as sites of T cell priming, activation and modulation, leading us to speculate that the interaction between metastatic cancer cells and T cells in lymph nodes may be distinct compared to other sites of metastases. However, no statistical differences were observed in relation

to lymph node involvement (Supplementary Fig. 3d-f). Taken together, these data suggest differences in T cell response based on anatomical site, that is, T cell exclusion, suppression and a more focused T cell response in proximity to the primary tumor.

**Distinct T cell repertoire profiles are associated with left-side thoracic tumors**

To evaluate T-cell responses in the tumors, we next focused on the most prevalent TCR clonotypes. Distinct clonotypes were detected in left-side thoracic tumors (left lung tumor, left pleural cavity, left hilar lymph node and left parietal pleura) compared to others. This result was intriguing considering bilateral pneumonia and leukocytosis were observed, though more inflammation was noted in the left thoracic cavity than the right. Strikingly, the most prevalent clonotype in “other” tumors (*CACR-PGNEAFF*) was entirely undetectable in left-side thoracic tumors (P, M02, M03 and M04) (Fig. 2e). Similar trends were also observed among the top 5 and 10 TCR clonotypes with certain clonotypes completely excluded from left-side thoracic tumors (Supplementary Fig. 4a-b). These data illustrate spatial restriction even among



the most prevalent T cell clonotypes across synchronous metastases.

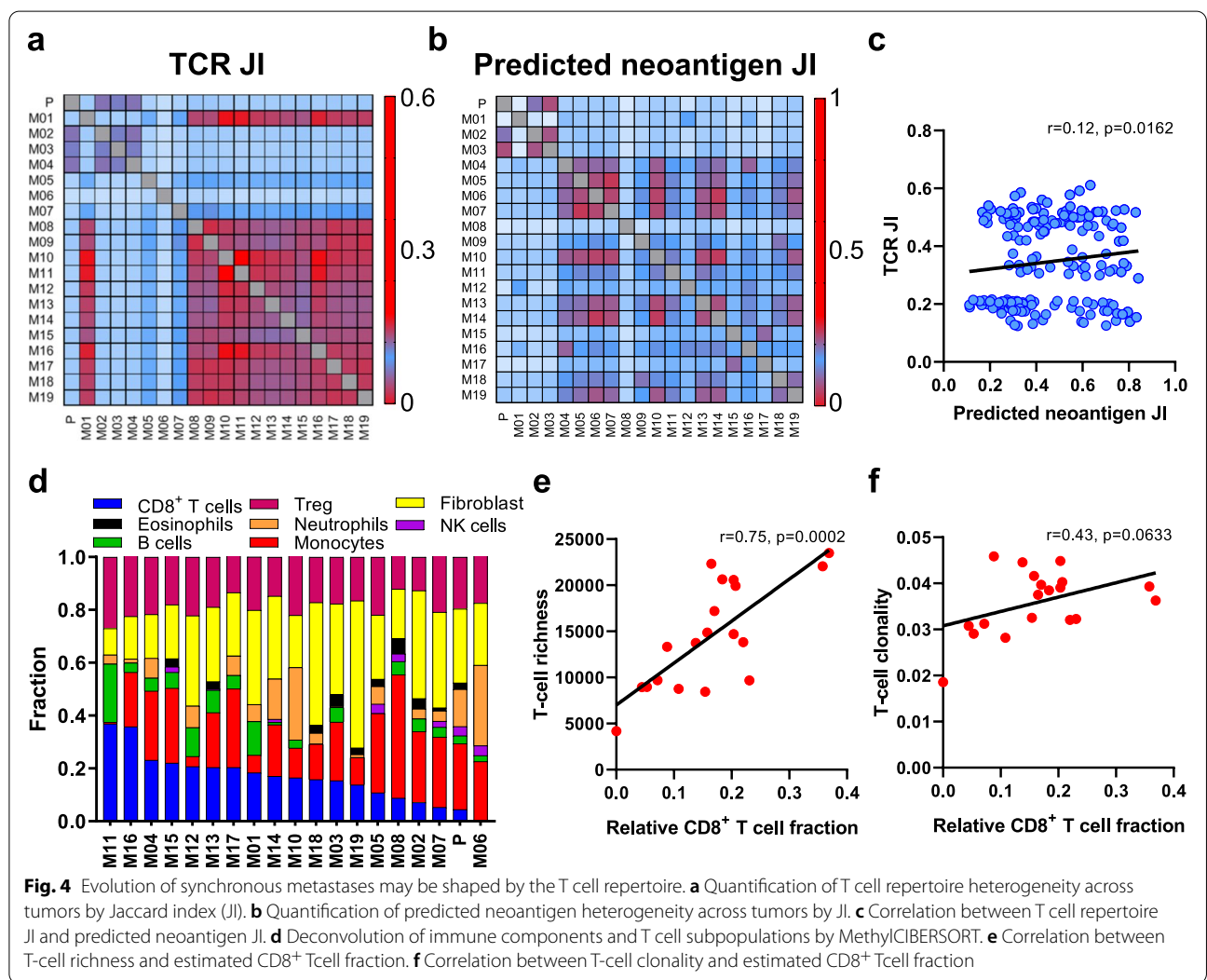
**T cell repertoire heterogeneity is observed across differentially growing tumors**

To gain deeper insights into TCR heterogeneity, we assessed the overlap between T cell repertoires across different tumors. We first compared the proportion (JI) and frequency of T cell clonotypes shared between the primary tumor and metastases. In accordance with the unique T cell clonotype pattern observed in tumors from the left side thorax, proportions and frequencies of shared T cells were much more similar between the three left thoracic metastases (M02, M03 and M04) and primary tumor (P) (Fig. 3a-c). T cell repertoire heterogeneity was evident across all tumors, with an average JI value of 0.35 (ranging from 0.12 to 0.61) and more shared T cells between proximal tumors (Fig. 4a), significantly higher than in a previously published cohort of 11 multi-region localized non-small cell lung cancers (NSCLCs) [44]

(average 0.35 vs. 0.17,  $p < 0.0001$ ) (Supplementary Fig. 5). Next, we studied the proportion and frequency of shared T cell clonotypes across all 20 tumors. In total, 599 T-cell clones were shared across all tumors, with proportions ranging from 3.0 to 15.4% (average = 5.39%) and frequencies accounting for 11.9% to 21.5% of the T cell repertoire (average = 15.96%) (Supplementary Fig. 6a-b). Of interest, both a greater proportion ( $p < 0.01$ ) and percentage ( $p < 0.01$ ) of shared T cell clones were observed in thoracic tumors compared to non-thoracic tumors (Supplementary Fig. 6c-d).

**Evolution of synchronous metastases may be shaped by the T cell repertoire**

We next performed *in silico* prediction of HLA-A-, -B-, and -C-presented neoantigens using NetMHC3.4 [26–28]. On average, 39 predicted neoantigens ( $IC_{50} < 500$  nmol/L) were detected per tumor, with the most ( $n = 60$ ) seen in the primary tumor and fewest ( $n = 20$ ) in the thyroid gland. Only 11 high binding affinity



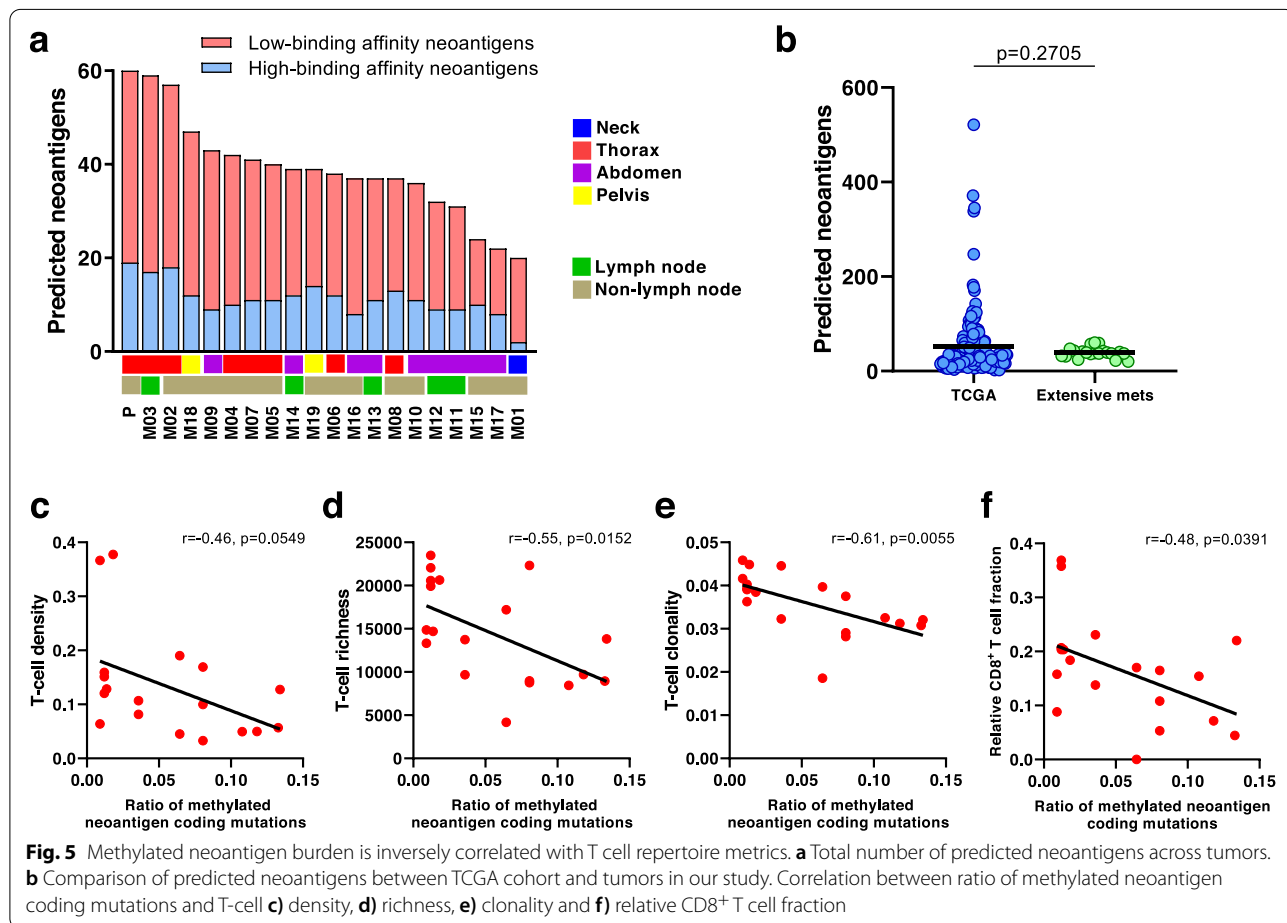
neoantigens were detected on average ( $IC_{50} < 50$  nmol/L) with the most ( $n=19$ ) also in the primary tumor and least ( $n=2$ ) in the thyroid gland (Fig. 5a). This falls within range but below the average of 53 predicted neoantigens seen in non-smokers from TCGA (Fig. 5b). We then evaluated the relationship between the T cell repertoire and predicted neoantigens. Predicted neoantigen heterogeneity was also evident, with the average JI value of 0.44 (ranging from 0.11 to 0.84, Fig. 4b), and a weak but statistically-significant positive correlation between T cell repertoire and neoantigen homology ( $r=0.12$ ,  $p=0.0162$ , Fig. 4c), which could suggest the distribution of T cells may be partially driven by their reactivity to shared neoantigens. Interestingly, ratio of methylated neoantigen coding mutations was negatively associated with T-cell density ( $r=-0.46$ ,  $p=0.0549$ ), richness ( $r=-0.55$ ,  $p=0.0152$ ) and clonality ( $r=-0.61$ ,  $p=0.0055$ ) (Fig. 5c-e), suggesting neoantigen methylation may contribute to immune suppression and potentially explaining the weak neoantigen associations with T cell repertoire homology.

To assess immune infiltration, we next performed cellular deconvolution analyses using MethylCIBERSORT (Fig. 4d) [32]. Unfortunately, no distinct immune

cell infiltration patterns were noted in left-side thoracic tumors (P, M02, M03 and M04) (Supplementary Fig. 7). However, relative  $CD8^+$  T cell fraction was correlated with richness ( $r=0.75$ ,  $p=0.0002$ ) and clonality ( $r=0.43$ ,  $p=0.063$ ) (Fig. 4e, f). Furthermore, CD8 to Treg ratio, which correlates with a more favorable outcome in cancer [45, 46], was also correlated with T-cell richness ( $r=0.68$ ,  $p=0.0012$ ) and clonality ( $r=0.64$ ,  $p=0.032$ ) (Supplementary Fig. 8a-b). A negative correlation between  $CD8^+$  T cell fraction and methylated neoantigen coding mutations was also observed ( $r=-0.48$ ,  $p=0.0391$ , Fig. 5e). These results highlight the greater proliferative potential of  $CD8^+$  T cells and suggest T cell reactivity and diversity may be mainly driven by the clonal expansion of  $CD8^+$  T cells at the patient level, as previously suggested by our group and others [47]. Overall, our findings suggest that the evolution of synchronous metastases may be shaped by the T cell response in absence of prior therapy.

### Discussion

Metastasis is an evolutionary process shaped by the dynamic interactions between tumor cells and host factors including immune surveillance [48]. T cells play



a pivotal role in mediating this process by recognizing antigens presented on MHC molecules at the surface of tumors and carrying out cytotoxic responses against tumor cells harboring their cognate antigens [49]. Accordingly, much importance has been attributed to T cell infiltration in many solid tumors, with more T cells generally associated with a better prognosis [39, 50, 51]. However, recent studies have highlighted the impact of intratumor heterogeneity (ITH) and bystander T cells [52–54], and suggested that only ~10% of tumor-infiltrating lymphocytes are capable of recognizing antigens presented by the tumor they have infiltrated [55], prompting deeper investigations into the T cell repertoire. Our understanding of the role of genomic and immune heterogeneity in lung cancer has evolved in recent years, thanks to investigations by our group and others into differences between regions of individual tumors, synchronous metastases and between primary and metastatic tumors [44, 56–59] highlighting potential spatial and temporal factors influencing clinical outcomes [60, 61]. Here, we assess the characteristics of the T cell repertoire in a treatment-naïve non-smoking patient with synchronous lung metastases and depict the interplay between the primary tumor and synchronous metastases [11, 44, 62], revealing extensive immunogenomic intertumor heterogeneity across primary and metastatic sites.

In our study, clonal *TP53* mutations were detectable in all tumors, suggestive of an early genomic event, in line with prior reports [24, 63]. Interestingly, a higher overlap in somatic mutations was observed across proximal tumors suggesting they are more genetically similar, potentially due to metastatic seeding from the primary tumor [64, 65]. Though our study focused on a single patient, the overlap in mutational burden observed between synchronous metastases is in line with previous reports in lung [59], melanoma [66], kidney [67] and colon cancer [68]. Considering the role of somatic mutations in triggering T cell responses through the generation of neoantigens, this overlap suggests these somatic mutations may serve as potential therapeutic targets for vaccination or T cell engineering through targeting of unifying antigens present across all synchronous tumors. This is supported by the modest but significant correlation between shared mutations and shared TCRs though additional studies are needed to confirm these hypotheses.

We observed lower T cell repertoire heterogeneity across synchronous metastases in our study than in our prior work assessing multi-region ITH of localized LUAD [44]. This difference could highlight the distinct resistance mechanisms at play in accelerated progression in our study versus more gradual progression in early-stage LUAD which may have allowed for divergent genomic evolution and immune editing over years. This

is reinforced by the absolute restriction of certain T cell clonotypes to metastases surrounding the primary tumor, which could be reflective of the distinct antigenic environments established in distal tumors. Unfortunately, our lack of deep immune phenotyping data precludes our ability to further investigate the role the distinct immune microenvironments, including chemokine gradients and receptors, which may have played a role in establishing these vastly distinct T cell microenvironments. However, the presence of shared T cell clonotypes could also be indicative of common responses against unifying antigens displayed across synchronous metastases.

Aberrant methylation has been reported to be involved in tumorigenesis in a variety of cancers and its impact on anti-tumor immune surveillance are very complex [69–72]. DNA methylation could affect immune surveillance directly by regulating the expression of potential neoantigens and/or immune-related genes thereby suppressing anti-tumor immune responses [73] or indirectly via modifying chromosomal vulnerability for mutations and copy number alterations (CNAs), both of which are well known to influence the tumor immune microenvironment [74–76]. A high level of hypomethylation could also lead to a high CNA burden which has been associated with a cold tumor immune microenvironment therefore facilitating immune evasion. Conversely, a high level of hypomethylation is associated with an increased mutational burden, which could increase tumor immunogenicity [74]. However, in the end, the selected cancer cell clones of late-metastases could escape immunosurveillance through the cumulative effects of these molecular aberrations. Recently, considerable progress has been reported in the identification of protein factors with a highly conserved DNA interaction surface, termed the methyl CpG-binding domain (MBD) [77]. MBD proteins could couple DNA methylation to transcriptional repression therefore silencing tumor suppressor genes that are hypermethylated at their promoter CpG islands in cancer cells [77]. MBD1 silences the *IRF8* gene, which is a central mediator in the  $\text{IFN}\gamma/\text{STAT1}$  signaling pathway governing the establishment of immune responses [78]. Therefore, disrupting MBD1-mediated silencing could enhance immune surveillance. Interestingly, in the current study, the ratio of methylated neoantigen coding mutations was negatively associated with T-cell density, richness and clonality, even at an individual level. One could therefore hypothesize that therapeutic agents modulating methylation could potentially reprogram the immune microenvironment and could exhibit some potential in treating these tumors.

Our study does exhibit certain limitations, including its focus on a single patient. However, analysis of several synchronous tumor sites from a single patient with advanced

disease in absence of heavy pre-treatment is rarely possible due to the lack of clinical indication. Unfortunately, deeper analysis of underlying mechanisms, immune cells and soluble factors influencing T cell trafficking and heterogeneity remain unclear due to the archival nature of these samples and will require further investigation. It is well known that DNA methylation is involved in differentiation and activation of naïve CD4<sup>+</sup> T cells [79, 80]. DNA methylation could release gene suppression upon demethylation of promoter regions regulating differential Th1 and Th2 cytokine secretion and therefore interrupting CD4<sup>+</sup> T-cell polarization with effector phenotypes in these cells [81, 82]. Interestingly, up to 27% of methylated genes in promoter regions are actively expressed in naïve CD4<sup>+</sup> T cells and associated with immune response and T cell differentiation [83]. Moreover, a recent study by Bam M *et al* [84] found that the majority of differentially methylated regions (DMRs) in tumor CD4<sup>+</sup> T cells are located in the promoters followed by intergenic regions and introns. One could therefore assume that methylated genes in intergenic regions are also involved in naïve CD4<sup>+</sup> T cell polarization and differentiation into specific lineages. Unfortunately, we were unable to investigate the impact of DNA methylation on the immune system and how genes in promoters or intergenic regions regulate CD4<sup>+</sup> T cell differentiation and activation in our cohort due to a lack of metastasis-paired normal tissue controls.

Despite these limitations, our study provides important evidence of differential tumor-immune responses co-existing in metastases within the same individual, related not only to molecular alterations. As a result, our findings may also partially explain the challenge of treating late-stage lung cancer due to the heterogeneity of metastases. Additional genomic, transcriptomic and immune studies in patients with synchronous metastases could help shed light on these and other mechanisms at play and provide therapeutic insights into late-stage NSCLC. Lastly, our study demonstrates heterogeneous immunogenomic profiles across synchronous metastases and provides important evidence of differential tumor-immune responses co-existing in metastases within the same individual, partially resulting in the challenge of treating late-stage lung cancer. These results advocate for combination regimens with drugs exhibiting distinct mechanisms of action, e.g. concurrent chemotherapy with immunotherapy or anti-PD-1 plus anti-CTLA-4 [85] to eradicate cancer cells displaying different immunogenomic features to improve survival of patients with synchronous lung cancer metastases [66]. Ideally, biopsies of multiple sites should be considered when feasible

to identify common neoantigens across different disease sites, which could be targeted therapeutically. Interestingly, a shared TP53 mutation was identified across all tumor lesions and the patient was found to express HLA-A\*02:01. Recent work has revealed that TP53-derived neoantigens can be targeted using Bispecific T cell Engagers (BiTEs), highlighting a potentially effective therapeutic option for this patient [86]. Under most circumstances, however, multi-site biopsy is not clinically safe or practical. Alternatively, canonical cancer gene alterations, which are often present in all cancer across different sites [87], are appropriate targets. Moreover, with the caveat of variable detection sensitivity, liquid biopsy is less impacted by tumor heterogeneity [88, 89], and may therefore provide a holistic view of molecular features across different metastatic sites to complement molecular profiling from tumor biopsies.

## Conclusion

In summary, in this study, we present the heterogeneous immunogenomic landscape of one primary tumor and 19 synchronous metastases from a minimally-pretreated young female never-smoker with late-stage LUAD. Only a TP53 mutation was detected in all tumors suggesting it was an early genomic event while other cancer gene mutations occurred at later times. Fewer less diverse and reactive T cells infiltrated the metastases nearest to the primary tumor, and a set of prevalent T cell clonotypes were excluded from left-side thoracic tumors further suggesting immune escape near the primary site. Furthermore, shared predicted neoantigens were associated with homology of the T cell repertoire across metastases. Lastly, ratio of methylated neoantigen coding mutations was negatively associated with T-cell density, richness and clonality, suggesting neoantigen methylation may partially drive immunosuppression. Our study demonstrates heterogeneous genomic and T cell profiles across synchronous metastases and how restriction of unique T cell clonotypes within an individual may differentially shape the genomic and epigenomic landscapes of synchronous lung metastases.

## Abbreviations

BiTEs: Bispecific T cell engagers; CNAs: Copy number alterations; CT: Computed tomography; DMRs: Differentially methylated regions; H&E: Hematoxylin and eosin; ITH: Intratumor heterogeneity; JI: Jaccard index; LUAD: Lung adenocarcinoma; MBD: Methyl CpG-binding domain; MRI: Magnetic resonance imaging; SNVs: Single nucleotide variants; SWAN: Subset-quantile within-array normalization; TCR: T cell receptor; WES: Whole-exome sequencing; VAF: Variant allele frequency.

## Supplementary Information

The online version contains supplementary material available at <https://doi.org/10.1186/s13046-022-02361-x>.

**Additional file 1: Supplementary Figure 1.** Distinct mutational profiles are seen across primary tumor and synchronous metastases. **Supplementary Figure 2.** Distinct T cell repertoire metrics between tumors from patients in localized non-small cell lung cancer (NSCLC, PROSPECT cohort) and our patient. **Supplementary Figure 3.** Distinct T cell repertoire metrics between thoracic and non-thoracic tumors but no differences in relation to lymph node involvement. **Supplementary Figure 4.** Distinct antigenic profiles are associated with left-side thoracic tumors. **Supplementary Figure 5.** A higher TCR Jaccard index (JI) in our patient compared to a previously published multi-region localized non-small cell lung cancer (NSCLC). **Supplementary Figure 6.** Characterization of shared T cell clonotype proportions and percentages by all 20 tumors. **Supplementary Figure 7.** Immune cell fractions in left-side thoracic tumors versus non-left side thoracic tumors. **Supplementary Figure 8.** Positive correlations of CD8 to Treg ratio with TCR metrics. **Supplementary Table S1.** Sample information. **Supplementary Data.** TCR rearrangements.

### Additional file 2.

### Acknowledgements

Not applicable.

### Authors' contributions

A.R., D.L.G., L.A.B. and J.J.Z. conceived the study. R.C. and J.L. led the data analysis. J.F, D.T., and C.W.C. led the pathological assessment, multi-region sample preparation and DNA extraction. R.C., K.Q., L.H. and M.T. collected resected specimens and clinical data. L.L. and C.G. performed DNA preparation and whole-exome sequencing. X.S. and J.H.Z. performed sequencing raw data processing. J.L., X.H., K.Q., M.T. and A.M. performed downstream bioinformatics analyses. R.C., C.B, P.J., J.V.H., I.W., P.A.F., D.L.G., L.A.B., J.J.Z. and A.R. interpreted the data for clinical and pathological correlation. R.C. and J.L. performed statistical analyses. R.C., J.J.Z. and A.R. wrote the paper. All authors edited the manuscript. The authors read and approved the final manuscript.

### Funding

This work was supported by Conquer Cancer Foundation ASCO Young Investigator Award, MD Anderson Physician Scientist Award, Cancer Prevention & Research Institute of Texas (CPRIT) Multiple Investigator Award, TJ Martell Foundation, NIH/NCI R01-CA207295, NIH/NCI U01-CA213273 and Department of Defense (LC170171). A.R. was supported by the Exon 20 Group, Rexanna's Foundation for Fighting Lung Cancer, the Waun Ki Hong Lung Cancer Research Fund, MD Anderson's Lung Cancer Moon Shot, the Petrin Fund, the University Cancer Foundation via the Institutional Research Grant program at the University of Texas MD Anderson Cancer Center, the Happy Lungs Project, RETpositive, LUNGevity and the Cancer Prevention & Research Institute of Texas (RP210137). A.M. was supported by CPRIT Research Training Program (RP170067)

### Availability of data and materials

Data available upon request.

### Declarations

#### Ethics approval and consent to participate

Collection and use of patient samples were approved by the Institutional Review Board of the University of Texas MD Anderson Cancer Center.

#### Consent for publication

Not applicable.

#### Competing interests

L.A.B. serves on advisory committees for AstraZeneca, AbbVie, GenMab, BergenBio, Pharma Mar SA, Sierra Oncology, Merck, Bristol Myers Squibb, Genentech, and Pfizer and has research support from AbbVie, AstraZeneca, GenMab, Sierra Oncology and Tolero Pharmaceuticals. I.W. reports consulting

or advisory roles for AstraZeneca/MedImmune, Bayer, Bristol-Myers Squibb, Genentech/Roche, GlaxoSmithKline, Guardant Health, HTG Molecular Diagnostics, Merck, MSD Oncology, OncoCyte, Jansen, Novartis, Flame Inc, and Pfizer; has received grants and personal fees from Genentech/Roche, Bristol Myers Squibb, AstraZeneca/MedImmune, HTG Molecular, Merck, and Guardant Health; has received personal fees from GlaxoSmithKline and OncoCyte, Daiichi-Sankyo, Roche, Astra Zeneca, Pfizer and Bayer; has received research funding to his institution from 4D Molecular Therapeutics, Adaptimmune, Adaptive Biotechnologies, Akoya Biosciences, Amgen, Bayer, EMD Serono, Genentech, Guardant Health, HTG Molecular Diagnostics, Iovance Biotherapeutics, Johnson & Johnson, Karus Therapeutics, MedImmune, Merck, Novartis, OncoPlex Diagnostics, Pfizer, Takeda, and Novartis. J.J.Z. reports research funding from Merck, Johnson and Johnson, and consultant fees from BMS, Johnson and Johnson, AstraZeneca, Geneplus, OrigMed and Innovent outside the submitted work. J.V.H. reports honorariums from AstraZeneca, Boehringer-Ingelheim, Catalyst, Genentech, GlaxoSmithKline, Guardant Health, Foundation medicine, Hengrui Therapeutics, Eli Lilly, Novartis, Spectrum, EMD Serono, Sanofi, Takeda, Mirati Therapeutics, BMS, BrightPath Biotherapeutics, Janssen Global Services, Nexus Health Systems, EMD Serono, Pneuma Respiratory, Kairos Venture Investments, Roche and Leads Biolabs. A.R. serves on the Scientific Advisory Board and has received honoraria from Adaptive Biotechnologies. A.M. is an employee and receives stock/has ownership interests in Guardant Health. The other authors declare no competing interests.

### Author details

<sup>1</sup>Department of Thoracic/Head and Neck Medical Oncology, the University of Texas MD Anderson Cancer Center, Houston, TX 77030, USA. <sup>2</sup>Department of Genomic Medicine, the University of Texas MD Anderson Cancer Center, Houston, TX 77030, USA. <sup>3</sup>Department of Radiation Oncology, Sun Yat-sen University Cancer Center, State Key Laboratory of Oncology in South China, Collaborative Innovation Center for Cancer Medicine, Sun Yat-sen University, Guangzhou 510060, Guangdong, China. <sup>4</sup>Regor Therapeutics, 2445 Main Street, Second Floor, MA 02142 Cambridge, USA. <sup>5</sup>Department of Translational Molecular Pathology, the University of Texas MD Anderson Cancer Center, Houston, TX 77030, USA. <sup>6</sup>Department of Pathology, the University of Texas MD Anderson Cancer Center, Houston, TX 77030, USA.

Received: 15 October 2021 Accepted: 10 April 2022

Published online: 11 May 2022

### References

1. Tan WL, Jain A, Takano A, Newell EW, Iyer NG, Lim WT, et al. Novel therapeutic targets on the horizon for lung cancer. *Lancet Oncol*. 2016;17(8):e347–e62.
2. Negrao MV, Quek K, Zhang J, Sepesi B. TRACERx: Tracking tumor evolution to impact the course of lung cancer. *J Thorac Cardiovasc Surg*. 2018;155(3):1199–202.
3. Nowell PC. The clonal evolution of tumor cell populations. *Science*. 1976;194(4260):23–8.
4. Valastyan S, Weinberg RA. Tumor metastasis: molecular insights and evolving paradigms. *Cell*. 2011;147(2):275–92.
5. Yates LR, Campbell PJ. Evolution of the cancer genome. *Nat Rev Genet*. 2012;13(11):795–806.
6. Quek K, Li J, Estecio M, Zhang J, Fujimoto J, Roarty E, et al. DNA methylation intratumor heterogeneity in localized lung adenocarcinomas. *Oncotarget*. 2017;8(13):21994–2002.
7. Galon J, Bruni D. Tumor immunology and tumor evolution: intertwined histories. *Immunity*. 2020;52(1):55–81.
8. De Visser KE, Eichten A, Coussens LM. Paradoxical roles of the immune system during cancer development. *Nat Rev Cancer*. 2006;6(1):24–37.
9. Schreiber RD, Old LJ, Smyth MJ. Cancer immunoediting: integrating immunity's roles in cancer suppression and promotion. *Science*. 2011;331(6024):1565–70.
10. Dunn GP, Old LJ, Schreiber RD. The three Es of cancer immunoediting. *Annu Rev Immunol*. 2004;22:329–60.
11. McGranahan N, Furness AJ, Rosenthal R, Ramskov S, Lyngaa R, Saini SK, et al. Clonal neoantigens elicit T cell immunoreactivity and sensitivity to immune checkpoint blockade. *Science*. 2016;351(6280):1463–9.

12. Angelova M, Mlecnik B, Vasaturo A, Bindea G, Fredriksen T, Lafontaine L, et al. Evolution of metastases in space and time under immune selection. *Cell*. 2018;175(3):751–65.
13. Zhang AW, McPherson A, Milne K, Kroeger DR, Hamilton PT, Miranda A, et al. Interfaces of malignant and immunologic clonal dynamics in ovarian cancer. *Cell*. 2018;173(7):1755–69.
14. Jimenez-Sanchez A, Memon D, Pourpe S, Veeraraghavan H, Li Y, Vargas HA, et al. Heterogeneous tumor-immune microenvironments among differentially growing metastases in an ovarian cancer patient. *Cell*. 2017;170(5):927–38.
15. Shain AH, Bagger MM, Yu R, Chang D, Liu S, Vemula S, et al. The genetic evolution of metastatic uveal melanoma. *Nat Genet*. 2019;51(7):1123–30.
16. Menzies AM, Yeh I, Botton T, Bastian BC, Scolyer RA, Long GV. Clinical activity of the MEK inhibitor trametinib in metastatic melanoma containing BRAF kinase fusion. *Pigment Cell Melanoma Res*. 2015;28(5):607–10.
17. Sanborn JZ, Chung J, Purdom E, Wang NJ, Kakavand H, Wilmott JS, et al. Phylogenetic analyses of melanoma reveal complex patterns of metastatic dissemination. *Proc Natl Acad Sci U S A*. 2015;112(35):10995–1000.
18. Favero F, Joshi T, Marquard AM, Birkbak NJ, Krzystanek M, Li Q, et al. Sequenza: allele-specific copy number and mutation profiles from tumor sequencing data. *Ann Oncol*. 2015;26(1):64–70.
19. Cibulskis K, Lawrence MS, Carter SL, Sivachenko A, Jaffe D, Sougnez C, et al. Sensitive detection of somatic point mutations in impure and heterogeneous cancer samples. *Nat Biotechnol*. 2013;31(3):213–9.
20. Koboldt DC, Zhang Q, Larson DE, Shen D, McLellan MD, Lin L, et al. VarScan 2: somatic mutation and copy number alteration discovery in cancer by exome sequencing. *Genome Res*. 2012;22(3):568–76.
21. Kim S, Scheffler K, Halpern AL, Bekritsky MA, Noh E, Kallberg M, et al. Strelka2: fast and accurate calling of germline and somatic variants. *Nat Methods*. 2018;15(8):591–4.
22. Robinson JT, Thorvaldsdottir H, Winckler W, Guttman M, Lander ES, Getz G, et al. Integrative genomics viewer. *Nat Biotechnol*. 2011;29(1):24–6.
23. Thorvaldsdottir H, Robinson JT, Mesirov JP. Integrative Genomics Viewer (IGV): high-performance genomics data visualization and exploration. *Brief Bioinform*. 2013;14(2):178–92.
24. Jamal-Hanjani M, Wilson GA, McGranahan N, Birkbak NJ, Watkins TBK, Veeriah S, et al. Tracking the evolution of non-small-cell lung cancer. *New Engl J Med*. 2017;376(22):2109–21.
25. Schliep KP. phangorn: phylogenetic analysis in R. *Bioinformatics*. 2011;27(4):592–3.
26. Lundegaard C, Lamberth K, Harndahl M, Buus S, Lund O, Nielsen M. NetMHC-3.0: accurate web accessible predictions of human, mouse and monkey MHC class I affinities for peptides of length 8–11. *Nucleic Acids Res*. 2008;36:W509–12.
27. Lundegaard C, Lund O, Nielsen M. Accurate approximation method for prediction of class I MHC affinities for peptides of length 8, 10 and 11 using prediction tools trained on 9mers. *Bioinformatics*. 2008;24(11):1397–8.
28. Nielsen M, Lundegaard C, Blicher T, Lamberth K, Harndahl M, Justesen S, et al. NetMHCpan, a method for quantitative predictions of peptide binding to any HLA-A and -B locus protein of known sequence. *PLoS One*. 2007;2(8):e796.
29. Turker MS. The establishment and maintenance of DNA methylation patterns in mouse somatic cells. *Semin Cancer Biol*. 1999;9(5):329–37.
30. De Meyer T, Bady P, Trooskens G, Kurscheid S, Bloch J, Kros JM, et al. Genome-wide DNA methylation detection by MethylCap-seq and Infinium HumanMethylation450 BeadChips: an independent large-scale comparison. *Sci Rep*. 2015;5:15375.
31. Liu Y, Sethi NS, Hinoue T, Schneider BG, Cherniack AD, Sanchez-Vega F, et al. Comparative molecular analysis of gastrointestinal adenocarcinomas. *Cancer Cell*. 2018;33(4):721–35.
32. Chakravarthy A, Furness A, Joshi K, Ghorani E, Ford K, Ward MJ, et al. Pan-cancer deconvolution of tumour composition using DNA methylation. *Nat Commun*. 2018;9(1):3220.
33. Robins HS, Campreggher PV, Srivastava SK, Wacher A, Turtle CJ, Kahsai O, et al. Comprehensive assessment of T-cell receptor beta-chain diversity in alpha-beta T cells. *Blood*. 2009;114(19):4099–107.
34. Carlson CS, Emerson RO, Sherwood AM, Desmarais C, Chung MW, Parsons JM, et al. Using synthetic templates to design an unbiased multiplex PCR assay. *Nat Commun*. 2013;4:2680.
35. Robins H, Desmarais C, Matthias J, Livingston R, Andriesen J, Reijonen H, et al. Ultra-sensitive detection of rare T cell clones. *J Immunol Methods*. 2012;375(1–2):14–9.
36. Ding L, Getz G, Wheeler DA, Mardis ER, McLellan MD, Cibulskis K, et al. Somatic mutations affect key pathways in lung adenocarcinoma. *Nature*. 2008;455(7216):1069–75.
37. Imielinski M, Berger AH, Hammerman PS, Hernandez B, Pugh TJ, Hodis E, et al. Mapping the hallmarks of lung adenocarcinoma with massively parallel sequencing. *Cell*. 2012;150(6):1107–20.
38. Govindan R, Ding L, Griffith M, Subramanian J, Dees ND, Kanchi KL, et al. Genomic landscape of non-small cell lung cancer in smokers and never-smokers. *Cell*. 2012;150(6):1121–34.
39. Tumei H, Harview CL, Yearley JH, Shintaku IP, Taylor EJ, Robert L, et al. PD-1 blockade induces responses by inhibiting adaptive immune resistance. *Nature*. 2014;515(7528):568–71.
40. Cha E, Klinger M, Hou Y, Cummings C, Ribas A, Faham M, et al. Improved survival with T cell clonotype stability after anti-CTLA-4 treatment in cancer patients. *Sci Transl Med*. 2014;6(238):238ra70.
41. Reuben A, Gittelman R, Zhang J, Chen R, Quek K, Vence L, et al. OA 13.05 Immune, molecular and T cell repertoire landscape of 235 resected non-small cell lung cancers and paired normal lung tissues. *J Thorac Oncol*. 2017;12(11):S1780.
42. Gil Del Alcazar CR, Alečković M, Polyak K. Immune escape during breast tumor progression. *Cancer Immunol Res*. 2020;8(4):422–7.
43. Walker R, Poleszczuk J, Pilon-Thomas S, Kim S, Anderson A, Czerniecki BJ, et al. Immune interconnectivity of anatomically distant tumors as a potential mediator of systemic responses to local therapy. *Sci Rep*. 2018;8(1):9474.
44. Reuben A, Gittelman R, Gao J, Zhang J, Yusko EC, Wu CJ, et al. TCR repertoire intratumor heterogeneity in localized lung adenocarcinomas: an association with predicted neoantigen heterogeneity and postsurgical recurrence. *Cancer Discov*. 2017;7(10):1088–97.
45. Baras AS, Drake C, Liu J-J, Gandhi N, Kates M, Hoque MO, et al. The ratio of CD8 to Treg tumor-infiltrating lymphocytes is associated with response to cisplatin-based neoadjuvant chemotherapy in patients with muscle invasive urothelial carcinoma of the bladder. *Oncoimmunology*. 2016;5(5):e1134412.
46. Jordanova ES, Gorter A, Ayachi O, Prins F, Durrant LG, Kenter GG, et al. Human leukocyte antigen class I, MHC class I chain-related molecule A, and CD8+/regulatory T-cell ratio: which variable determines survival of cervical cancer patients? *Clin Cancer Res*. 2008;14(7):2028–35.
47. Qi Q, Liu Y, Cheng Y, Glanville J, Zhang D, Lee JY, et al. Diversity and clonal selection in the human T-cell repertoire. *Proc Natl Acad Sci U S A*. 2014;111(36):13139–44.
48. Labelle M, Hynes RO. The initial hours of metastasis: the importance of cooperative host–tumor cell interactions during hematogenous dissemination. *Cancer Discov*. 2012;2(12):1091–9.
49. Kitamura T, Qian B-Z, Pollard JW. Immune cell promotion of metastasis. *Nat Rev Immunol*. 2015;15(2):73–86.
50. Robert L, Tsoi J, Wang X, Emerson R, Homet B, Chodon T, et al. CTLA4 blockade broadens the peripheral T-cell receptor repertoire. *Clin Cancer Res*. 2014;20(9):2424–32.
51. Reuben A, Gittelman R, Zhang J, Quek K, Vence LM, Behrens C, et al. Association of the T-cell receptor landscape with survival in non-small cell lung cancer. *J Clin Oncol*. 2018;36(5):140.
52. Chiou S-H, Tseng D, Reuben A, Mallajosyula V, Molina IS, Conley S, et al. Global analysis of shared T cell specificities in human non-small cell lung cancer enables HLA inference and antigen discovery. *Immunity*. 2021;54(3):586–602.
53. Reuben A, Zhang J, Chiou SH, Gittelman RM, Li J, Lee WC, et al. Comprehensive T cell repertoire characterization of non-small cell lung cancer. *Nat Commun*. 2020;11(1):603.
54. Simoni Y, Becht E, Fehlings M, Loh CY, Koo S-L, Teng KWW, et al. Bystander CD8+ T cells are abundant and phenotypically distinct in human tumour infiltrates. *Nature*. 2018;557(7706):575–9.
55. Scheper W, Kelderman S, Fanchi LF, Linnemann C, Bendle G, de Rooij MA, et al. Low and variable tumor reactivity of the intratumoral TCR repertoire in human cancers. *Nat Med*. 2019;25(1):89–94.

56. Zhang J, Fujimoto J, Zhang J, Wedge DC, Song X, Zhang J, et al. Intratumor heterogeneity in localized lung adenocarcinomas delineated by multiregion sequencing. *Science*. 2014;346(6206):256–9.
57. Lee WC, Reuben A, Hu X, McGranahan N, Chen R, Jalali A, et al. Multiomics profiling of primary lung cancers and distant metastases reveals immunosuppression as a common characteristic of tumor cells with metastatic plasticity. *Genome Biol*. 2020;21(1):271.
58. Hong L, Negrão MV, Dibaj SS, Chen R, Reuben A, Bohac JM, et al. Programmed death-ligand 1 heterogeneity and its impact on benefit from immune checkpoint inhibitors in NSCLC. *J Thorac Oncol*. 2020;15(9):1449–59.
59. Liu Y, Zhang J, Li L, Yin G, Zhang J, Zheng S, et al. Genomic heterogeneity of multiple synchronous lung cancer. *Nat Commun*. 2016;7:13200.
60. Kim R, Keam B, Kim S, Kim M, Kim SH, Kim JW, et al. Differences in tumor microenvironments between primary lung tumors and brain metastases in lung cancer patients: therapeutic implications for immune checkpoint inhibitors. *BMC Cancer*. 2019;19(1):19.
61. Vignot S, Frampton GM, Soria JC, Yelensky R, Commo F, Brambilla C, et al. Next-generation sequencing reveals high concordance of recurrent somatic alterations between primary tumor and metastases from patients with non-small-cell lung cancer. *J Clin Oncol*. 2013;31(17):2167–72.
62. Zhang J, Fujimoto J, Zhang J, Wedge DC, Song X, Zhang J, et al. Intratumor heterogeneity in localized lung adenocarcinomas delineated by multiregion sequencing. *Science*. 2014;346(6206):256–9.
63. Leong TL, Gayevskiy V, Steinfort DP, De Massy MR, Gonzalez-Rajal A, Marini KD, et al. Deep multi-region whole-genome sequencing reveals heterogeneity and gene-by-environment interactions in treatment-naïve, metastatic lung cancer. *Oncogene*. 2019;38(10):1661–75.
64. Cheung KJ, Ewald AJ. A collective route to metastasis: Seeding by tumor cell clusters. *Science*. 2016;352(6282):167–9.
65. Heyde A, Reiter JG, Naxerova K, Nowak MA. Consecutive seeding and transfer of genetic diversity in metastasis. *Proc Natl Acad U S A*. 2019;116(28):14129–37.
66. Reuben A, Spencer CN, Prieto PA, Gopalakrishnan V, Reddy SM, Miller JP, et al. Genomic and immune heterogeneity are associated with differential responses to therapy in melanoma. *NPJ Genom Med*. 2017;2:10.
67. Becerra MF, Reznik E, Redzematovic A, Tennenbaum DM, Kashan M, Ghanaat M, et al. Comparative genomic profiling of matched primary and metastatic tumors in renal cell carcinoma. *Eur Urol Focus*. 2018;4(6):986–94.
68. Lim B, Mun J, Kim JH, Kim CW, Roh SA, Cho DH, et al. Genome-wide mutation profiles of colorectal tumors and associated liver metastases at the exome and transcriptome levels. *Oncotarget*. 2015;6(26):22179–90.
69. Ehrlich M. DNA hypomethylation in cancer cells. *Epigenomics*. 2009;1(2):239–59.
70. Park C, Jeong K, Park JH, Jung S, Bae JM, Kim K, et al. Pan-cancer methylation analysis reveals an inverse correlation of tumor immunogenicity with methylation aberrancy. *Cancer Immunol Immunother*. 2021;70(6):1605–17.
71. Hu X, Estecio MR, Chen R, Reuben A, Wang L, Fujimoto J, et al. Evolution of DNA methylome from precancerous lesions to invasive lung adenocarcinomas. *Nat Commun*. 2021;12(1):687.
72. Dejima H, Hu X, Chen R, Zhang J, Fujimoto J, Parra ER, et al. Immune evolution from preneoplasia to invasive lung adenocarcinomas and underlying molecular features. *Nat Commun*. 2021;12(1):2722.
73. Rosenthal R, Cadieux EL, Salgado R, Al Bakir M, Moore DA, Hiley CT, et al. Neoantigen-directed immune escape in lung cancer evolution. *Nature*. 2019;567(7749):479–85.
74. Liu M, Zhou J, Chen Z, Cheng AS. Understanding the epigenetic regulation of tumours and their microenvironments: opportunities and problems for epigenetic therapy. *J Pathol*. 2017;241(1):10–24.
75. Jung H, Kim HS, Kim JY, Sun JM, Ahn JS, Ahn MJ, et al. DNA methylation loss promotes immune evasion of tumours with high mutation and copy number load. *Nat Commun*. 2019;10(1):4278.
76. Davoli T, Uno H, Wooten EC, Elledge SJ. Tumor aneuploidy correlates with markers of immune evasion and with reduced response to immunotherapy. *Science*. 2017;355(6322):eaaf8399.
77. Parry L, Clarke AR. The roles of the methyl-CpG binding proteins in cancer. *Genes Cancer*. 2011;2(6):618–30.
78. Lopez-Serra L, Ballestar E, Fraga MF, Alaminos M, Setien F, Esteller M. A profile of methyl-CpG binding domain protein occupancy of hypermethylated promoter CpG islands of tumor suppressor genes in human cancer. *Cancer Res*. 2006;66(17):8342–6.
79. Coit P, Dozmorov MG, Merrill JT, McCune WJ, Maksimowicz-McKinnon K, Wren JD, et al. Epigenetic reprogramming in naïve CD4+ T cells favoring T cell activation and non-Th1 effector T cell immune response as an early event in lupus flares. *Arthritis Rheum*. 2016;68(9):2200–9.
80. O'Shea JJ, Paul WE. Mechanisms underlying lineage commitment and plasticity of helper CD4+ T cells. *Science*. 2010;327(5969):1098–102.
81. Lee GR, Kim ST, Spilianakis CG, Fields PE, Flavell RA. T helper cell differentiation: regulation by cis elements and epigenetics. *Immunity*. 2006;24(4):369–79.
82. Caiafa P, Zampieri M. DNA methylation and chromatin structure: the puzzling CpG islands. *J Cell Biochem*. 2005;94(2):257–65.
83. Hughes T, Webb R, Fei Y, Wren J, Sawalha A. DNA methylome in human CD4+ T cells identifies transcriptionally repressive and non-repressive methylation peaks. *Genes Immun*. 2010;11(7):554–60.
84. Bam M, Chintala S, Fetcko K, Williamsen BC, Siraj S, Liu S, et al. Genome wide DNA methylation landscape reveals glioblastoma's influence on epigenetic changes in tumor infiltrating CD4+ T cells. *Oncotarget*. 2021;12(10):967–81.
85. Gandhi L, Rodríguez-Abreu D, Gadgeel S, Esteban E, Felip E, De Angelis F, et al. Pembrolizumab plus chemotherapy in metastatic non-small-cell lung cancer. *N Engl J Med*. 2018;378(22):2078–92.
86. Hsueh EH-C, Wright KM, Douglass J, Hwang MS, Mog BJ, Pearlman AH, et al. Targeting a neoantigen derived from a common TP53 mutation. *Science*. 2021;371(6533):eabc8697.
87. Lee W-C, Reuben A, Hu X, McGranahan N, Chen R, Jalali A, et al. Multiomics profiling of primary lung cancers and distant metastases reveals immunosuppression as a common characteristic of tumor cells with metastatic plasticity. *Genome Biol*. 2020;21(1):271.
88. Nong J, Gong Y, Guan Y, Yi X, Yi Y, Chang L, et al. Circulating tumor DNA analysis depicts subclonal architecture and genomic evolution of small cell lung cancer. *Nat Commun*. 2018;9(1):3114.
89. Lam VK, Zhang J, Wu CC, Tran HT, Li L, Diao L, et al. Genotype-specific differences in circulating tumor DNA levels in advanced NSCLC. *J Thorac Oncol*. 2021;16(4):601–9.

## Publisher's Note

Springer Nature remains neutral with regard to jurisdictional claims in published maps and institutional affiliations.

Ready to submit your research? Choose BMC and benefit from:

- fast, convenient online submission
- thorough peer review by experienced researchers in your field
- rapid publication on acceptance
- support for research data, including large and complex data types
- gold Open Access which fosters wider collaboration and increased citations
- maximum visibility for your research: over 100M website views per year

At BMC, research is always in progress.

Learn more [biomedcentral.com/submissions](https://biomedcentral.com/submissions)

